Persistent aberrant cortical phase–amplitude coupling following seizure treatment in absence epilepsy models

Atul Maheshwari[1] (iD), Abraham Akbar[1], Mai Wang[1,2], Rachel L. Marks[1], Katherine Yu[1,2], Suhyeorn Park[1], Brett L. Foster[3,4] and Jeffrey L. Noebels[1,4,5]

[1]*Department of Neurology, Baylor College of Medicine, Houston, TX, USA*
[2]*Rice University, Houston, TX, USA*
[3]*Department of Neurosurgery, Baylor College of Medicine, Houston, TX, USA*
[4]*Department of Neuroscience, Baylor College of Medicine, Houston, TX, USA*
[5]*Department of Molecular and Human Genetics, Baylor College of Medicine, Houston, TX, USA*

The Journal of Physiology

Key points

- In two monogenic models of absence epilepsy, interictal beta/gamma power is augmented in homozygous *stargazer* (*stg*/*stg*) but not homozygous *tottering* (*tg*/*tg*) mice.
- There are distinct gene-linked patterns of aberrant phase–amplitude coupling in the interictal EEG of both *stg*/*stg* and *tg*/*tg* mice, compared to +/+ and *stg*/+ mice.
- Treatment with ethosuximide significantly blocks seizures in both genotypes, but the abnormal phase–amplitude coupling remains.
- Seizure-free *stg*/+ mice have normal power and phase–amplitude coupling, but beta/gamma power is significantly reduced with NMDA receptor blockade, revealing a latent cortical network phenotype that is separable from, and therefore not a result of, seizures.
- Altogether, these findings reveal gene-linked quantitative electrographic biomarkers free from epileptiform activity, and provide a potential network correlate for persistent cognitive deficits in absence epilepsy despite effective treatment.

Abstract In childhood absence epilepsy, cortical seizures are brief and intermittent; however there are extended periods without behavioural or electrographic ictal events. This genetic disorder is associated with variable degrees of cognitive dysfunction, but no consistent functional biomarkers that might provide insight into interictal cortical function have been described. Previous work in monogenic mouse models of absence epilepsy have shown that the interictal EEG displays augmented beta/gamma power in homozygous *stargazer* (*stg*/*stg*) mice bearing a presynaptic AMPA receptor defect, but not homozygous *tottering* (*tg*/*tg*) mice with a P/Q type calcium channel mutation. To further evaluate the interictal EEG, we quantified phase–amplitude coupling (PAC) in *stg*/*stg*, *stg*/+, *tg*/*tg* and wild-type (+/+) mice. We found distinct gene-linked patterns of aberrant PAC in *stg*/*stg* and *tg*/*tg* mice compared to +/+ and *stg*/+ mice. Treatment with ethosuximide significantly blocks seizures in both *stg*/*stg* and *tg*/*tg*, but the abnormal PAC remains. *Stg*/+ mice are seizure free with normal baseline beta/gamma power and normal theta-gamma PAC, but like *stg*/*stg* mice, beta/gamma power is significantly reduced by NMDA receptor blockade, a treatment that paradoxically enhances seizures in *stg*/*stg* mice. *Stg*/+ mice, therefore, have a latent cortical network phenotype that is veiled by NMDA-mediated neurotransmission. Altogether, these findings reveal gene-linked quantitative electrographic biomarkers in the absence of epileptiform activity and provide a potential network correlate for persistent cognitive deficits in absence epilepsy despite effective treatment.

Introduction

Childhood absence epilepsy is a genetic seizure disorder characterized by frequent spontaneous episodes of behavioural arrest associated with generalized spike-wave discharges in the electroencephalogram (EEG). Some patients with absence epilepsy also have neurocognitive deficits that are known to persist despite effective pharmacological seizure treatment (Masur *et al.* 2013). This suggests that genetic mutations responsible for the epileptic phenotype may also be independently responsible for cognitive deficits even without the presence of seizures. Therefore, even though the interictal EEG is generally considered to appear clinically normal, closer examination beyond standard electrographic markers may yield abnormalities that serve as biomarkers for underlying gene-linked cortical dysfunction. For example, augmented high frequency oscillations have been reported in patients with childhood absence epilepsy using magnetoencephalography (Xiang *et al.* 2014).

The homozygous *stargazer (stg/stg)* and *tottering (tg/tg)* mouse models of absence epilepsy are due to distinct monogenic mutations. *stg/stg* mice bear a mutation in *Cacng2* leading to AMPA receptor trafficking dysfunction in a subset of inhibitory neurons (Noebels *et al.* 1990; Barad *et al.* 2012; Maheshwari *et al.* 2013), and a mutation in the *tg/tg* gene *Cacna1a* impairs neurotransmitter release within the thalamocortical circuit (Noebels & Sidman, 1979; Rossignol *et al.* 2013; Bomben *et al.* 2016). We have previously found that *stg/stg* mice have significantly elevated interictal beta and gamma power, in contrast to *tg/tg* mice, which have normal power across frequencies between 2 and 300 Hz (Maheshwari *et al.* 2016). Therefore, a simple change in baseline EEG power alone is not a uniform finding in absence epilepsy and therefore may not selectively reflect genetic dysfunction or the potential neurocognitive deficits experienced by patients with absence epilepsy.

Another potential EEG biomarker of circuit level dynamics is cross-frequency coupling (Canolty & Knight, 2010). One common type of cross-frequency coupling is phase–amplitude coupling (PAC) where the phase of a slower oscillation is correlated with the amplitude of a faster oscillation. The magnitude of PAC represents the putative interactions between underlying circuits which behave abnormally in models of focal epilepsy (Guirgis *et al.* 2015; Amiri *et al.* 2016; Edakawa *et al.* 2016), but has not yet been evaluated in generalized epilepsies. Critically, PAC is a potentially useful metric as the correlation between different oscillatory EEG components may vary without overt changes in the power spectrum, and can therefore uniquely differ for similar power spectra. Here we examine the relationship between genetic mutations, absence epilepsy and PAC in the interictal EEG. We show that even in the absence of epileptiform activity, there are reproducible electrographic biomarkers of genetic dysfunction.

Methods

Ethical approval

Experiments were carried out according to the guidelines laid down by the Baylor Institutional Animal Care and Use Committee (IACUC) and conform to the principles and regulations of *The Journal of Physiology* (Grundy, 2015). Mice were adult (> 6 weeks old) homozygous *stargazer* (*stg/stg*) and *tottering* (*tg/tg*) mutants, heterozygous *stargazer* mice (*stg/+*), and wild-type (*+/+*) mice of either sex, originally obtained from The Jackson Laboratory (Bar Harbor, Maine) and maintained on a C57BL6/J background for over 10 generations. Genotypes were confirmed by PCR of tail DNA (Burgess & Noebels, 1999). For electrode implantation, mice were anaesthetized by tribromoethanol (Avertin; 20 μl g^{-1} I.P.) or isoflurane (2–4% in O_2) anaesthesia and surgically implanted with silver wire electrodes (0.127 mm diameter) inserted into the epidural space over the somatosensory cortex (1 mm posterior and 3 mm lateral to bregma) bilaterally through cranial burr holes and attached to a microminiature connector cemented to the skull. The reference electrode was placed over the right frontal lobe (1 mm anterior and 1 mm lateral to bregma) and the ground electrode was placed over the left frontal lobe. Mice were allowed to recover for at least 2 weeks prior to recording. Access to food and water was available *ad libitum*. If necessary, mice were euthanized by CO_2 inhalation using an automated CO_2 delivery system (SmartBox, Euthanex, Palmer, PA, USA).

Video-EEG data recording

EEG and behavioural activity in freely moving mice were recorded using simultaneous video-EEG monitoring (Harmonie software version 6.1c, Stellate Systems, Natus Medical, Pleasanton, CA, USA). All *in vivo* experiments were performed between 12.00 and 15.00 h to prevent confounding diurnal variation (Smyk *et al.* 2011). EEG signals were sampled at 2 kHz with an anti-aliasing filter. Prior to recording, mice were allowed to acclimate to the recording environment for 30 min, and video-EEG was then collected for a 30 min sampling period (the baseline period for both power and PAC analysis), followed by intraperitoneal drug injection. Drug effect was analysed between 30 and 60 min after drug administration.

Video-EEG data pre-processing

Investigators were blinded to genotype and drug administered prior to data analysis. EEG data were then

screened for seizure activity under the supervision of a board-certified epileptologist (A.M.). Seizures were defined by episodes of bilateral spike and wave discharges with amplitude greater than or equal to 1.5× baseline voltage and concomitant video-recorded behavioural arrest. EEGs were reviewed without knowledge of genotype or treatment, and any recording artefacts were removed from analysis. Since the power of high frequency oscillations may be falsely measured when there are sharp electrographic contours (Kramer *et al.* 2008; Scheffer-Teixeira *et al.* 2013), identified seizure episodes were digitally extracted in EEGLab (Delorme & Makeig, 2004) to allow evaluation of only interictal activity periods. Raw data were notch filtered with a 1 Hz window around 60, 120 and 180 Hz using EEGLab (Delorme & Makeig, 2004) in MATLAB (Mathworks, Inc., Natick, MA, USA).

Phase–amplitude coupling analysis

PAC analyses were performed in EEGLab (Delorme & Makeig, 2004), Brainstorm (Tadel *et al.* 2011) and custom routines (MATLAB). The pre-processed inter-ictal EEG was analysed independently in both left and right recording leads. The right parietal lead was used for further analysis, unless there was significant artefact, in which case the left recording lead was used. Baseline PAC was evaluated in Brainstorm by creating a PAC comodulogram with frequencies of 2–30 Hz for phase (*x*-axis) and 30–200 Hz for amplitude (*y*-axis). The PAC algorithm in Brainstorm uses the mean vector length method of determining a 'direct PAC' measure (Özkurt & Schnitzler, 2011). Given significant PAC dependence on state (Scheffzük *et al.* 2011), animals with peak direct PAC below 10^{-2} indicated were excluded from the analysis. As a control measure, comodulograms were also estimated

using two other common methods: phase-locking value (Penny *et al.* 2008) and modulation index (Tort *et al.* 2010). As described below, these methods produced highly similar results as statistically assessed by rank correlation of comodulogram matrices between methods, and therefore the main analyses focused on the direct PAC estimation data. Comodulograms were then used to identify and compare peak PAC frequency pairs (phase and amplitude). Periods of active wakefulness were determined by exporting segments of EEG that corresponded to locomotor activity on simultaneous video recording.

Power analysis

Pre- and post-drug interictal EEG power spectrum was estimated using the spectral analysis function (spectropo()) in EEGLab (Delorme & Makeig, 2004). Left and right recording leads were analysed separately for power between 2 and 200 Hz with a window size of 8 s and a window overlap of 6 s; AP was then averaged across both leads. Relative power (RP) was calculated by dividing the absolute power values for each frequency by the total power (TP; 2–200 Hz), and then normalized with a log transformation before comparison between mice (RP = AP/TP), similar to methods previously described (Koopman *et al.* 1996; Jobert *et al.* 2012).

Drugs

Ethosuximide (Sigma-Aldrich, St Louis, MO, USA) and the NMDA antagonist MK-801 (Tocris Bioscience, Minneapolis, MN, USA) were first dissolved in DMSO, brought to 1% volume/weight of each animal being tested in a phosphate-buffered saline solution (Thermo Fisher Scientific, Waltham, MA, USA), and then injected intraperitoneally.
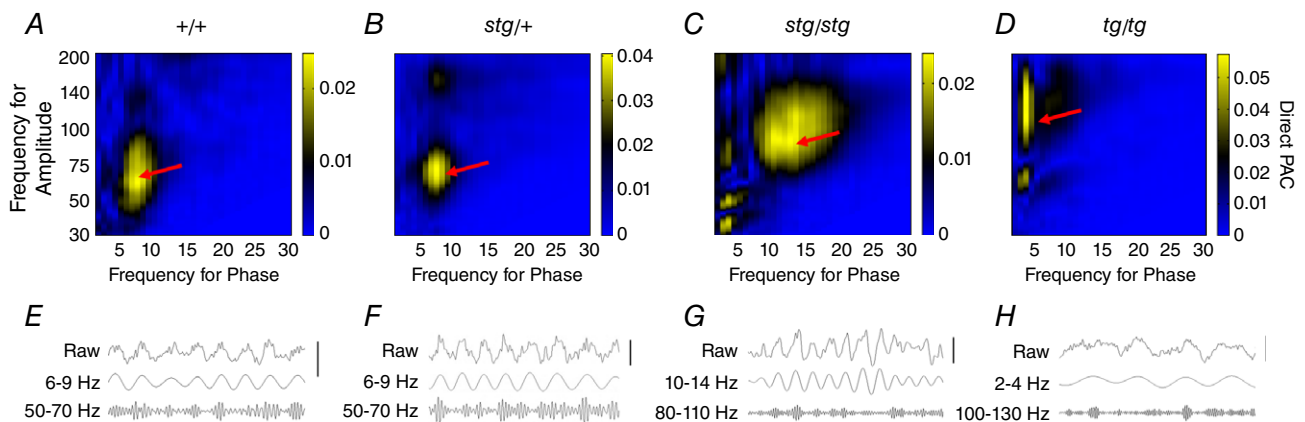
Figure 1. Representative examples of PAC in +/+, *stg*/+, *stg*/*stg*, and *tg*/*tg* mice
Comodulograms showed prominent theta–gamma coupling in +/+ and *stg*/+ mice. In contrast, there was maximal PAC with alpha/beta–high gamma coupling in *stg*/*stg* mice, and maximal PAC with delta–high gamma coupling in *tg*/*tg* mice (A–D, red arrows). One second of raw seizure-free data traces is displayed in E–H (vertical bar, 100 μV for raw and low frequency traces, 300 μV for high frequency traces).

Statistics

The statistical significance of peak PAC pairs was estimated using circular data shuffling to create 2000 surrogates for comparison via a Rayliegh test at $P < 0.05$. Group analysis of the resultant data was performed using a one-way repeated measures ANOVA with Tukey's test for multiple comparisons (for baseline studies) or Wilcoxon's test (for drug studies), and the adjusted significance was set at $P < 0.05$. Comparisons between maximum PAC, phase for frequency and phase for amplitude before and after medication administration was analyzed with a Student's paired t-test. Finally, given the clear differences observed in mean PAC comodulograms between animal groups (see below), we explored the utility of PAC profiles to identify group similarity between single animals in an unsupervised data driven manner. Similar to the PAC method comparison above, comodulograms for each animal were transformed into vectors and correlated (Spearman's rank correlation). This correlation/similarity matrix (comprising all animals) was then converted to a dissimilarity matrix (1 − correlation value). Multidimensional scaling (MDS) was then applied to the dissimilarity matrix to visualize the PAC based similarity

of each animal (where geometric distance conveys similarity). These analytic steps are highly similar to representational similarity analysis commonly performed in functional brain imaging (Kriegeskorte *et al.* 2008).

For power analysis, statistical differences between groups at baseline were tested using a two-way ANOVA with Dunnett's *post hoc* test comparing to +/+ at each frequency. Differences due to drug exposure were tested using a repeated-measures two-way ANOVA to compare groups before and after drug administration with Sidak's *post hoc* test at each frequency. Statistical significance was set at an adjusted $P < 0.05$ at two or more consecutive frequencies to avoid spurious significance. All statistical analysis was performed using Prism version 7.01 (GraphPad Software, La Jolla, CA, USA).

Results

Gene-specific shift in maximal phase amplitude coupling in stargazer and tottering mice

Comodulograms between the phase of 2–30 Hz and the amplitude of 30–200 Hz were created for +/+,
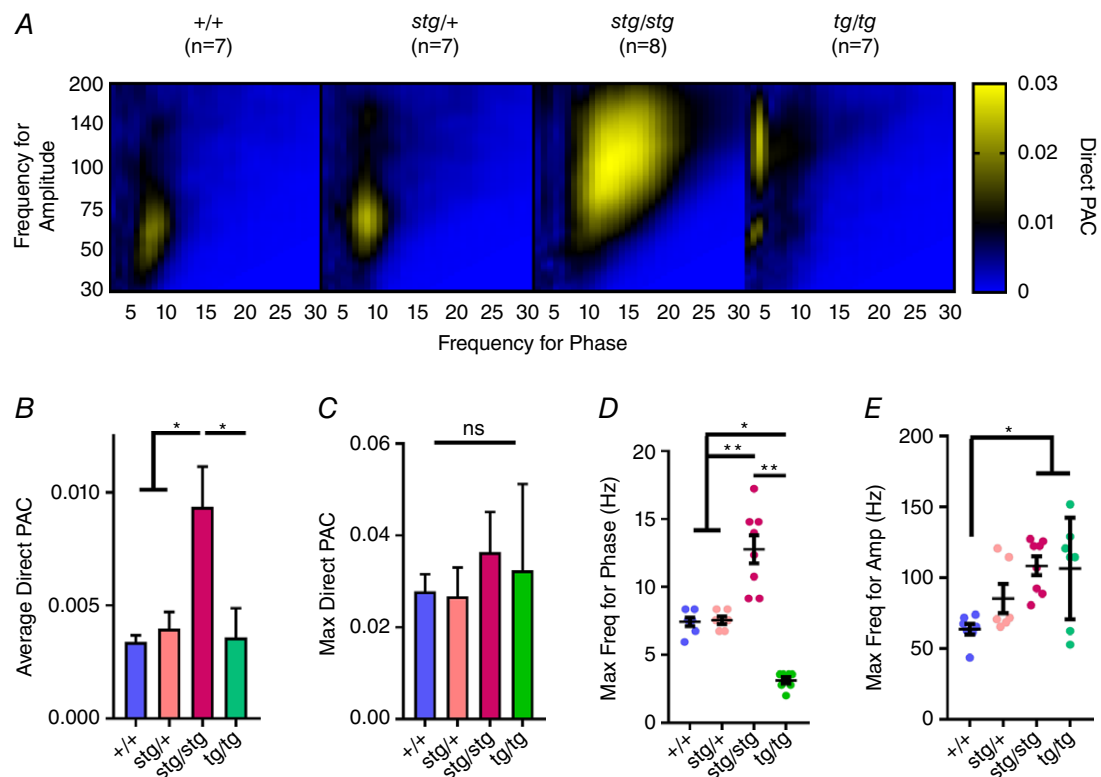
Figure 2. Gene-specific shifts in the PAC comodulogram
A, average comodulograms for +/+, *stg*/+, *stg*/*stg* and *tg*/*tg* mice reveal distinct abnormal patterns in both homozygous mutants. *B*, increased average direct PAC in *stg*/*stg* mice compared to all other genotypes. *C*, no significant change in the maximum PAC. *D*, there is a significant shift to a greater phase frequency in *stg*/*stg* and to a lower phase frequency in *tg*/*tg* mice. *E*, there is a significant increase in the amplitude frequency in both *stg*/*stg* and *tg*/*tg* mice (one-way ANOVA with multiple comparisons, *adjusted $P < 0.05$, **adjusted $P < 0.005$).

stg/+, stg/stg and tg/tg mice using the baseline inter-ictal EEG. Sample PAC comodulograms are displayed in Fig. 1A–D. In wild-type and stg/+ mice, there was significant coupling between gamma oscillations at the peak of theta (Fig. 1A and E). In contrast, stg/stg mice showed maximal coupling between the phase of alpha/beta and high-gamma oscillations (Fig. 1C and G), while tg/tg

mice showed maximal coupling between the phase of delta and high-gamma oscillations (Fig. 1D and H).

Group PAC data are shown in Fig. 2. There was no significant difference between +/+ and stg/+ mice in the average overall PAC, the maximum PAC value, maximum frequency for phase, or maximum frequency for amplitude. stg/stg mice had no difference in maximum
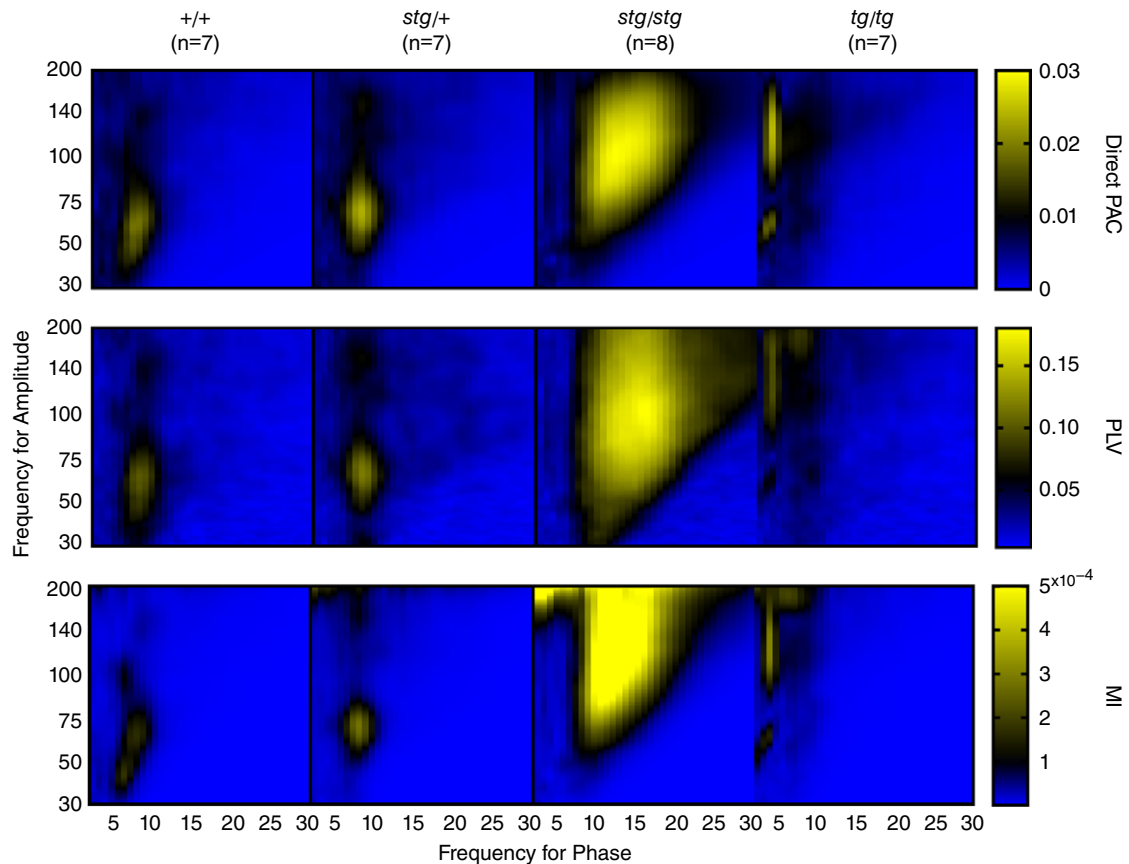

Figure 3. Similar comodulograms with different methods of calculating PAC: original Brainstorm method (direct PAC, top), phase-locking value (PLV, middle) and modulation index (MI, bottom)
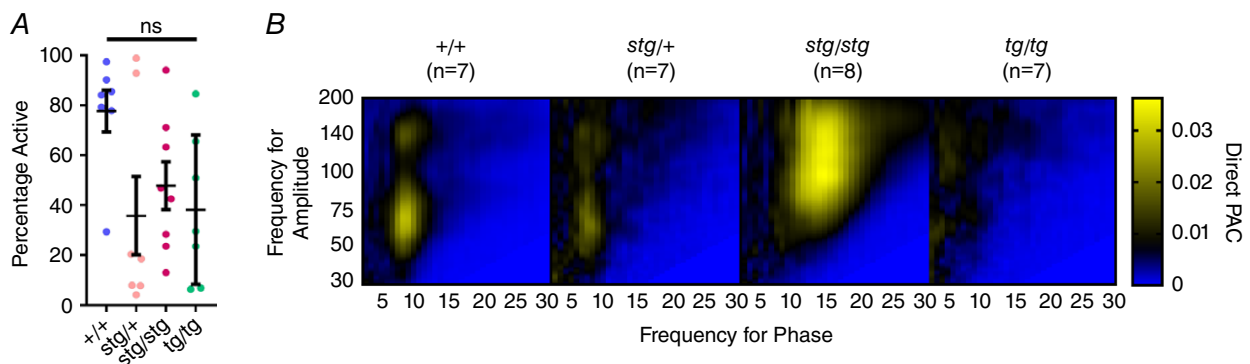

Figure 4. Similar comodulograms when evaluating only active wakefulness
A, no significant difference in the percentage of time in active wakefulness across genotypes. B, comodulograms show similar peak frequencies for phase and amplitude with shifts in stg/stg and tg/tg but not in stg/+ mice.

PAC value, but a significantly increased average PAC and increased frequencies for both peak phase and peak amplitude, shifting the peak in the comodulogram rightward and upward. *tg/tg* mice also had no difference in maximum PAC value and had no difference in average PAC. However, *tg/tg* mice did have significantly decreased peak frequency for phase and increased peak frequency for amplitude, shifting the comodulogram peak leftward and upward (Fig. 2*D* and *E*).

### Validation of phase–amplitude coupling

To ensure that group differences in mean PAC comodulograms were invariant to estimation method, we also calculated mean comodulograms using the phase-locking value (PLV; Penny *et al.* 2008) and modulation index (MI; Tort *et al.* 2010) techniques (see Methods). As seen in Fig. 3, all three methods of PAC estimation produce highly similar mean comodulograms. To quantify this similarity we performed rank-correlations (Spearman) on comodulograms between methods for each animal group. Both alternative PAC techniques

showed highly similar comodulogram profiles compared with the initial direct PAC method: (i) PLV *vs.* direct PAC (+/+ = 0.93, *stg/*+ = 0.92, *stg/stg* = 0.90, *tg/tg* = 0.96); (ii) MI *vs.* direct PAC (+/+ = 0.98, *stg/*+ = 0.97, *stg/stg* = 0.96, *tg/tg* = 0.99); all $P < 0.001$.

To ensure that state of arousal was not confounding the difference in PAC between genotypes, we next asked whether there was a significant difference between the time mice were actively wakeful during the baseline recordings. The activity was quite variable across all genotypes, ranging from 4.15% to 98.9% active, with no significant difference between groups (Fig. 4*A*). When only these blocks of active wakefulness were analysed, the maximum frequency for phase and frequency for amplitude were not significantly changed across all genotypes (Fig. 4*B*).

Persistent abnormal phase–amplitude coupling with ethosuximide

We next evaluated the degree of PAC before and after treating seizures with the antiepileptic drug ethosuximide, the preferred treatment for human childhood absence
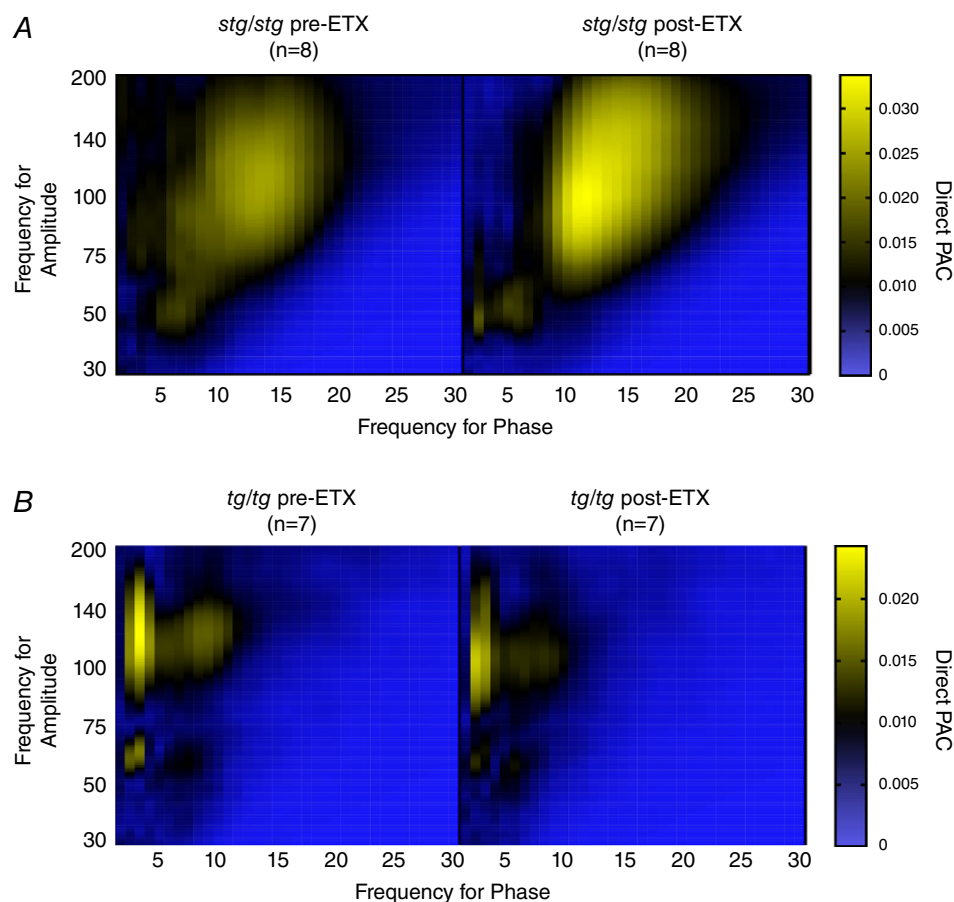

Figure 5. Persistent aberrant interictal PAC following abolition of seizures with ethosuximide in both *stg/stg* (A) and *tg/tg* mice (B)

epilepsy (Glauser *et al.* 2013). As we have shown previously, a 200 mg kg^{-1} intraperitoneal dose of ethosuximide significantly reduces seizure activity for several hours for both *stg/stg* and *tg/tg* mice (Maheshwari *et al.* 2013). Compared to the 30 min baseline period prior to injection, there was no observable change to the comodulogram between 30 and 60 min after injection (Fig. 5*A* and *B*). The average PAC, maximum PAC, maximum frequency for phase, and maximum frequency for amplitude all had no significant difference comparing pre- and post-injection (*stg/stg*, $n = 8$, *tg/tg*, $n = 7$, paired *t* test, $P > 0.05$, Fig. 5).

Comodulogram profiles partially cluster genetic groups

To explore the utility of comodulogram profiles as putative EEG biomarkers of genetic class at the single animal level, we performed unsupervised similarity analysis. We compared the similarity of PAC comodulograms between all animals, and visualized this comparison geometrically using MDS (see Methods). Consistent with the qualitative features of the mean comodulograms (Fig. 2), MDS reveals a clear dissociation of *stg/stg* mice from overlapping members of the +/+ and *stg/+* mice (Fig. 6). In addition, aberrant patterns in *tg/tg* mice were more distant from *stg/stg* mice, but partially overlapping with +/+ and *stg/+*, consistent with comodulogram features. These relatively clear genotypic differences in group membership predict the potential for more formal classification approaches and possible diagnostic utility utilizing PAC comodulogram features.
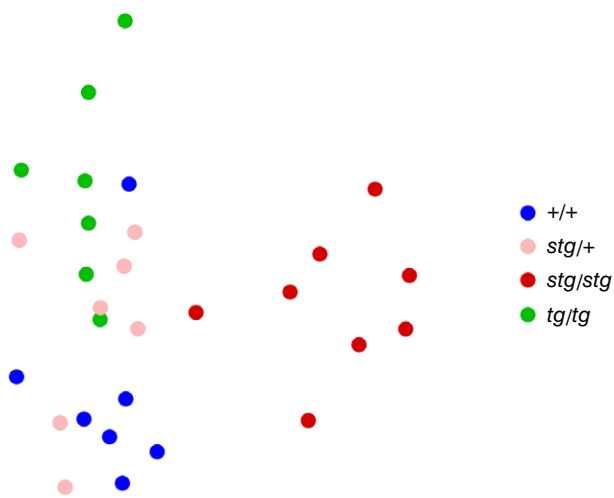
Figure 6. Group multidimensional scaling (MDS) plot showing distinct clustering of *stg/stg* away from *tg/tg*, +/+, and *stg/+* MDS was applied to a dissimilarity matrix (1 − Spearman rank correlation value) to visualize the PAC based similarity of each animal, where geometric distance conveys similarity (see Methods).

Heterozygous mice display no epilepsy with normal absolute and relative beta/gamma power

In all baseline recordings, +/+ and *stg/+* mice never exhibited seizures. Both *stg/+* ($n = 11$) and *tg/tg* ($n = 11$) mice had no significant change in baseline absolute power compared to +/+ ($n = 11$) mice, while *stg/stg* mice had significantly augmented absolute power between 11.25 and 39.5 Hz as well as 188.25–200 Hz (Fig. 7*A*). When correcting for total power, *stg/+* and *tg/tg* mice continued to have no significant difference from +/+ mice, but *stg/stg* mice had augmented 13.25–19.0 Hz relative power and a resultant reduction in 81.75–152.5 Hz relative power between 81.75 and 152.5 Hz (Fig. 7*B*).

Heterozygous stargazer mice display a reduction in beta/gamma power with NMDA receptor blockade

We previously found that the augmented beta/gamma power in *stg/stg* mice was reduced after administration of NMDA receptor blockade (Maheshwari *et al.* 2016), consistent with the hypothesis that impaired AMPA receptor trafficking in cortical parvalbumin-expressing neurons in *stg/stg* mice leads to an abnormal dependence on NMDA receptors to maintain these fast oscillations. Therefore, we next evaluated the response of *stg/+* to the NMDA antagonist MK-801 and found a response similar to *stg/stg* (Fig. 8), with both a reduction of beta/gamma power and the absence of a high gamma peak (150–180 Hz) that is seen in both +/+ and *tg/tg* mice. Therefore, despite freedom from seizures and a normal baseline gamma power, *stg/+* mice have electrographic abnormalities that are unmasked by NMDA receptor blockade. Altogether, these results are consistent with evidence that the AMPA receptor trafficking deficit, primarily located on cortical inter-neuron dendrites (Maheshwari *et al.* 2013), leads to an abnormal dependence on NMDA receptors for maintenance of beta/gamma power in *stg/+* mice.

Abnormal PAC response to NMDA receptor blockade in stargazer mice

Since MK-801 brought gamma power back down to normal levels in *stg/stg* mice, we next asked if NMDA receptor blockade could also normalize PAC. Overall, +/+, *stg/+* and *tg/tg* mice had a similar response, shifting the maximum PAC to an island centred in theta for phase and high-gamma for amplitude, whereas the maximum PAC in *stg/stg* mice shifted over to delta for phase and broad gamma for amplitude (Fig. 9*A*, *E* and *F*; $n = 6$ for each genotype). In +/+ mice, MK-801 caused the maximum direct PAC to increase to 0.102 ± 0.0133, significantly greater than the post-MK-801 maximum direct PAC in *stg/stg* (0.034 ± 0.009, mean $\pm$ SEM,

one-way ANOVA with Tukey's correction for multiple comparisons; adjusted $P = 0.0288$, Fig. 9*B*). While *stg/+* and *tg/tg* did not have as robust a response to MK-801 as *+/+*, only *stg/stg* had a significantly reduced change in maximum PAC (-0.001 ± 0.006) compared to *+/+* (0.079 ± 0.015, one-way ANOVA with Tukey's correction for multiple comparisons; adjusted $P = 0.0115$, Fig. 9*C*).

Discussion

In this study, we investigated whether oscillations within the EEG were significantly changed in mice with monogenic mutations associated with absence epilepsy in three states: (1) in the interictal state in *stg/stg* and *tg/tg* which have active epilepsy; (2) in treated epileptic mice which no longer have seizures; and (3) with *stg/+* mice which have
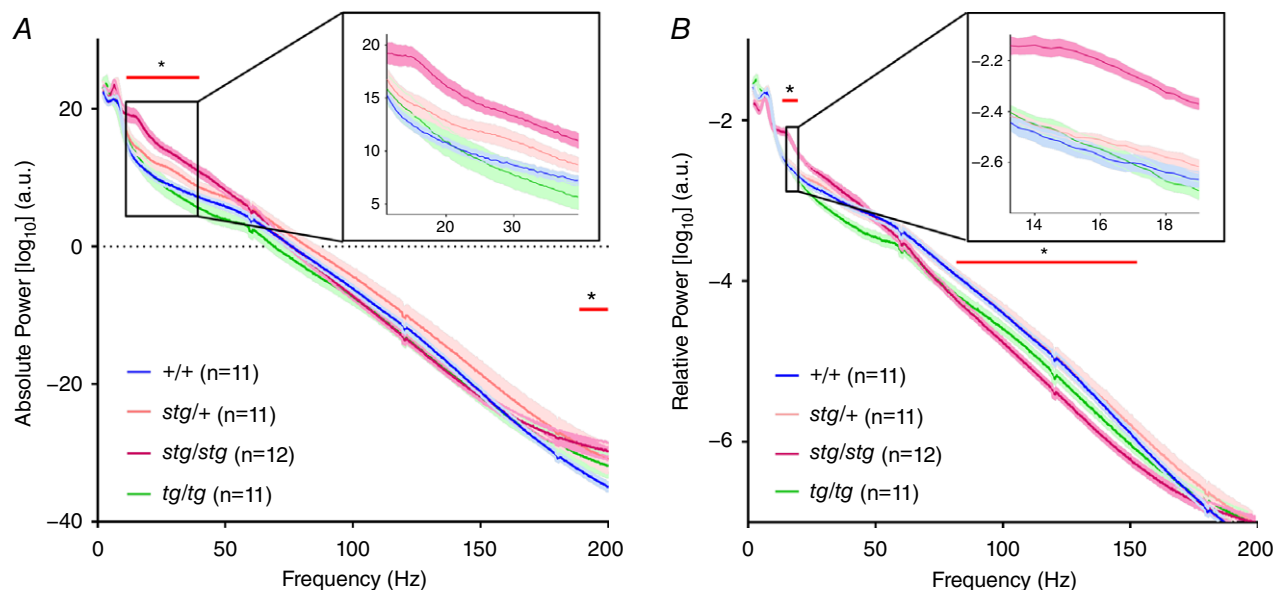
Figure 7. Mean ± SEM EEG power spectra for absolute and relative power
A, augmented absolute power in *stg/stg* compared to *+/+* mice between 11.25 and 39.5 Hz (inset) as well as 188.25–200 Hz. There is no significant difference in power at any frequency for *stg/+* or *tg/tg* mice. *B*, augmented relative power between 13.25 and 19 Hz in *stg/stg* mice compared to *+/+* mice with reduced relative power between 81.75 and 152.5 Hz. There is a non-significant trend toward augmented relative power in the delta range (3–4 Hz) for *tg/tg* compared to *+/+* (two-way ANOVA with Sidak's correction for multiple comparisons, *adjusted $P < 0.05$).
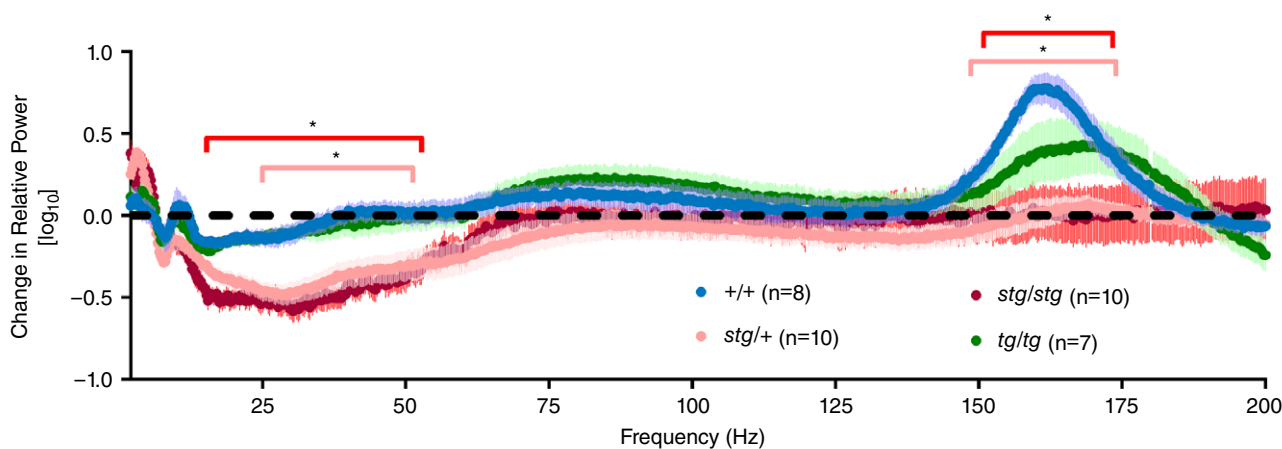
Figure 8. Change in relative power (mean ± SEM) with NMDA receptor blockade
The response to MK-801 in *stg/+* mice is similar to the response in *stg/stg* mice. Compared to *+/+*, both have significantly reduced relative power in the beta/gamma range (*stg/stg*, 15.25–53 Hz; *stg/+*, 24.75–51 Hz), with a lack of activation at high gamma range (*stg/stg*, 151.25–174.25 Hz; *stg/+*, 148.5–173.75 Hz, *adjusted $P < 0.05$). *tg/tg* mice respond to MK-801 in a similar manner to *+/+* mice (adjusted $P > 0.05$ at all frequencies).

no epilepsy. In each of these categories, we found potential EEG biomarkers for monogenic cortical dysfunction by evaluating absolute/relative power and phase–amplitude coupling at baseline and in response to medications.

Phase–amplitude coupling in *stg*/+ mice was unchanged compared to +/+ mice, showing prominent theta–gamma coupling. Theta–gamma coupling in parietal neocortex has been previously reported, predominantly in the awake state, with the greatest coupling occurring at the peak of the theta phase (Scheffzük *et al.* 2011). *stg/stg* and *tg/tg* mice, however,

both had significantly shifted interictal comodulograms compared to +/+ mice. *stg/stg* mice were significantly shifted rightward and upward, while *tg/tg* mice were significantly shifted leftward and upward. Since absolute and relative power were otherwise unaffected in *tg/tg* mice (Maheshwari *et al.* 2016), abnormal interictal PAC may have a greater association with absence epilepsy than abnormal baseline power. Further studies of interictal PAC in other models and patients with absence epilepsy are necessary to more thoroughly evaluate this hypothesis. Part of this confirmation should involve close
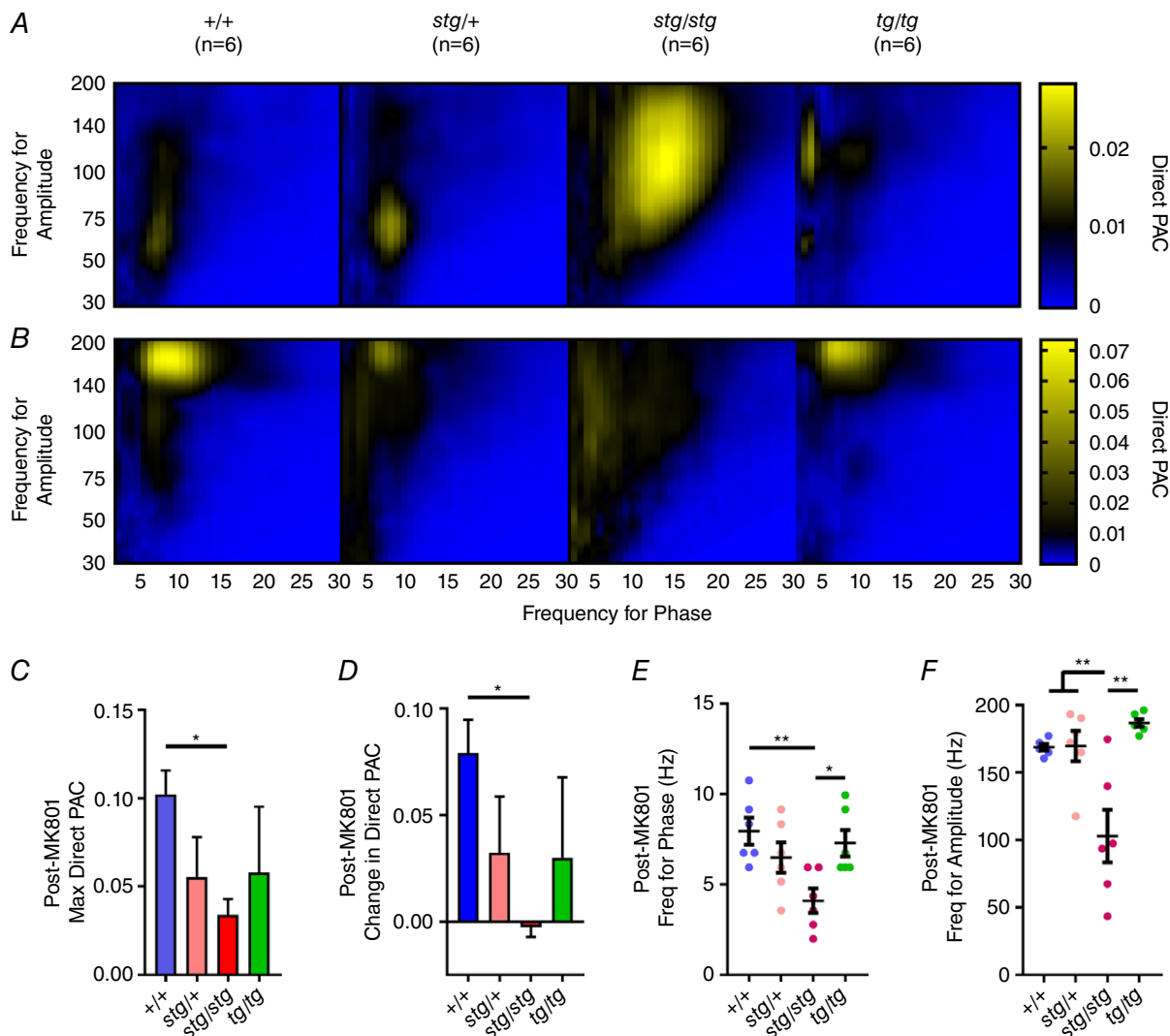
Figure 9. Change in PAC with NMDA receptor blockade
Compared to PAC before MK-801 (*A*), PAC after MK-801 (*B*) shifted to theta for phase and high-gamma for amplitude in all genotypes except for *stg/stg* mice. Note that the colour map range is adjusted to appreciate changes in comodulogram structure. *C*, the maximum direct PAC after MK-801 was significantly greater in +/+ than *stg/stg*, with intermediate responses in *stg*/+ and *tg/tg*. *D*, similarly, the change in direct PAC was significantly greater in +/+ than in *stg/stg* mice. *E*, frequency for phase shifted to delta for *stg/stg*, significantly lower than theta for phase in +/+ and *tg/tg*, and (*F*) frequency for amplitude for *stg/stg* was significantly lower than all other genotypes post-MK801 (*n* = 6 in each group, one-way ANOVA with Tukey's correction for multiple comparisons; *adjusted *P* < 0.05, **adjusted *P* < 0.01, **adjusted *P* < 0.0005).

consideration of EEG waveform morphology and its confounding influence on PAC estimation (Cole & Voytek, 2017). While sleep–wake cycles can also affect the degree of neocortical PAC in mice (Scheffzük *et al.* 2011), the shifts in phase–amplitude coupling remained when only periods of active wakefulness were examined (Fig. 4*B*). Nonetheless, a detailed analysis of the effect of brain state on interictal phase–amplitude coupling in epileptic mice is another important avenue of future research.

Treatment of seizures with ethosuximide in both genotypes did not significantly alter the underlying aberrant PAC. This finding suggests that the genetic mutations in these models, to some degree, generate abnormal circuit behaviour present during both the interictal and ictal states. Persistent abnormal PAC may underlie attention deficits in patients with absence epilepsy that are otherwise seizure-free after treatment of their epilepsy (Masur *et al.* 2013). This hypothesis is supported by recent work that correlates theta–gamma coupling with attention tasks in humans (Szczepanski *et al.* 2014) as well as impaired theta–gamma coupling in patients with attention deficit disorder (Kim *et al.* 2015). However, it is also possible that abnormal PAC and absence seizures are both epiphenomenal manifestations of underlying genetic dysfunction, without a causal link between abnormal PAC and deficits in attention. Further studies are necessary to dissect potential causal relationships between these phenomena.

Since we did not specifically test cognitive performance, we can only speculate as to the meaning of the shift in baseline PAC in the epileptic mice. Reduced theta–gamma coupling has been seen in amyloid precursor protein-deficient Alzheimer model mice (Zhang *et al.* 2016) and with reduced fast inhibition onto PV interneurons in the hippocampus (Wulff *et al.* 2009). However, a shift in PAC has not previously been seen specifically due to a genetic mutation. A shift in PAC has been seen in the consciousness transition with anaesthesia (Mukamel *et al.* 2014), and a shift from theta–gamma to alpha–gamma coupling has also been seen with visual tasks and attention (Voytek *et al.* 2010; Jensen *et al.* 2014). We hypothesize that the shifts we see in these mutant epileptic mice may be due to the specific effects of each genetic mutation on the underlying circuit responsible for phase–amplitude coupling (Onslow *et al.* 2014). Experiments modelling changes in cell type-specific connectivity have shown that theoretically these shifts can occur (Sotero, 2015).

Finally, *stg*/+ mice had no seizures and normal power. However, similar to *stg*/*stg* mice, *stg*/+ mice were found to have a significant drop in beta/gamma power with the NMDA receptor blocker MK-801. Therefore, despite the absence of electroclinical seizures, the EEG was able to reveal a biomarker for pharmacogenetic dysfunction when challenged with NMDA receptor blockade. In contrast to ethosuximide, which reduced seizure activity but had no

effect on PAC in *stg*/*stg* mice, MK-801 worsened seizures and significantly shifted PAC to the left. In +/+ mice, MK-801 shifted PAC from theta–gamma to theta–high gamma, which has been similarly shown in wild-type rats in response to ketamine, another NMDA receptor blocker (Cordon *et al.* 2015). Interestingly, PAC did not normalize to baseline +/+ levels, nor did it respond like +/+, but rather shifted to delta for phase and broadly over low and high gamma for amplitude. Since PAC in *tg*/*tg* responded similarly to +/+ in response to MK-801 which also significantly reduced seizures, we have shown that interictal PAC in mutant mice is not necessarily fixed, and there is a potential for pharmacologically shifting PAC while also concomitantly treating seizures.

With these experiments, we have demonstrated three different ways in which an EEG can show the potential for genetic dysfunction independent from seizures or any sharp activity. First, interictal PAC was abnormal at baseline in epileptic mice. Second, PAC remained abnormal despite pharmacological treatment with ethosuximide. Finally, heterozygous dysfunction was unmasked by a drop in beta/gamma power with NMDA receptor blockade. Therefore, when evaluating mouse models or patients with epilepsy, we have found that analysing both power and PAC, in addition to challenging subjects with various medications, is critical before declaring the interictal EEG as 'normal'.

References

Amiri M, Frauscher B & Gotman J (2016). Phase-amplitude coupling is elevated in deep sleep and in the onset zone of focal epileptic seizures. *Front Hum Neurosci* **10**, 387.

Barad Z, Shevtsova O, Arbuthnott GW & Leitch B (2012). Selective loss of AMPA receptors at corticothalamic synapses in the epileptic stargazer mouse. *Neuroscience* **217**, 19–31.

Bomben VC, Aiba I, Qian J, Mark MD, Herlitze S & Noebels JL (2016). Isolated P/Q calcium channel deletion in layer VI corticothalamic neurons generates absence epilepsy. *J Neurosci* **36**, 405–418.

Burgess DL & Noebels JL (1999). Single gene defects in mice: the role of voltage-dependent calcium channels in absence models. *Epilepsy Res* **36**, 111–122.

Canolty RT & Knight RT (2010). The functional role of cross-frequency coupling. *Trends Cogn Sci* **14**, 506–515.

Cole SR & Voytek B (2017). Brain oscillations and the importance of waveform shape. *Trends Cogn Sci* **21**, 137–149.

Cordon I, Nicolás MJ, Arrieta S, Lopetegui E, López-Azcárate J, Alegre M, Artieda J & Valencia M (2015). Coupling in the cortico-basal ganglia circuit is aberrant in the ketamine model of schizophrenia. *Eur Neuropsychopharmacol* **25**, 1375–1387.

Delorme A & Makeig S (2004). EEGLAB: an open source toolbox for analysis of single-trial EEG dynamics including independent component analysis. *J Neurosci Methods* **134**, 9–21.

Edakawa K, Yanagisawa T, Kishima H, Fukuma R, Oshino S, Khoo HM, Kobayashi M, Tanaka M & Yoshimine T (2016). Detection of epileptic seizures using phase-amplitude coupling in intracranial electroencephalography. *Sci Rep* **6**, 25422.

Glauser TA, Cnaan A, Shinnar S, Hirtz DG, Dlugos D, Masur D, Clark PO, Adamson PC & Childhood Absence Epilepsy Study Team (2013). Ethosuximide, valproic acid, and lamotrigine in childhood absence epilepsy: initial monotherapy outcomes at 12 months. *Epilepsia* **54**, 141–155.

Grundy D (2015). Principles and standards for reporting animal experiments in *The Journal of Physiology* and *Experimental Physiology*. *J Physiol* **593**, 2547–2549.

Guirgis M, Chinvarun Y, Del Campo M, Carlen PL & Bardakjian BL (2015). Defining regions of interest using cross-frequency coupling in extratemporal lobe epilepsy patients. *J Neural Eng* **12**, 026011.

Jensen O, Gips B, Bergmann TO & Bonnefond M (2014). Temporal coding organized by coupled alpha and gamma oscillations prioritize visual processing. *Trends Neurosci* **37**, 357–369.

Jobert M, Wilson FJ, Ruigt GSF, Brunovsky M, Prichep LS, Drinkenburg WHIM & IPEG Pharmaco-EEG Guidelines Committee (2012). Guidelines for the recording and evaluation of pharmaco-EEG data in man: The International Pharmaco-EEG Society (IPEG). *Neuropsychobiology* **66**, 201–220.

Kim JW, Lee J, Kim B-N, Kang T, Min KJ, Han DH & Lee YS (2015). Theta-phase gamma-amplitude coupling as a neurophysiological marker of attention deficit/hyperactivity disorder in children. *Neurosci Lett* **603**, 25–30.

Koopman PA, Wouters PA & Krijzer FN (1996). Mean power spectra from pharmaco-electrocorticographic studies: relative baseline correction and log transformation for a proper analysis of variance to assess drug effects. *Neuropsychobiology* **33**, 100–105.

Kramer MA, Tort ABL & Kopell NJ (2008). Sharp edge artifacts and spurious coupling in EEG frequency comodulation measures. *J Neurosci Methods* **170**, 352–357.

Kriegeskorte N, Mur M & Bandettini P (2008). Representational similarity analysis – connecting the branches of systems neuroscience. *Front Syst Neurosci* **2**, 4.

Maheshwari A, Marks RL, Yu KM & Noebels JL (2016). Shift in interictal relative gamma power as a novel biomarker for drug response in two mouse models of absence epilepsy. *Epilepsia* **57**, 79–88.

Maheshwari A, Nahm WK & Noebels JL (2013). Paradoxical proepileptic response to NMDA receptor blockade linked to cortical interneuron defect in stargazer mice. *Front Cell Neurosci* **7**, 156.

Masur D, Shinnar S, Cnaan A, Shinnar RC, Clark P, Wang J, Weiss EF, Hirtz DG, Glauser TA & Childhood Absence Epilepsy Study Group (2013). Pretreatment cognitive deficits and treatment effects on attention in childhood absence epilepsy. *Neurology* **81**, 1572–1580.

Mukamel EA, Pirondini E, Babadi B, Wong KFK, Pierce ET, Harrell PG, Walsh JL, Salazar-Gomez AF, Cash SS, Eskandar EN, Weiner VS, Brown EN & Purdon PL (2014). A transition in brain state during propofol-induced unconsciousness. *J Neurosci* **34**, 839–845.

Noebels JL, Qiao X, Bronson RT, Spencer C & Davisson MT (1990). Stargazer: a new neurological mutant on chromosome 15 in the mouse with prolonged cortical seizures. *Epilepsy Res* **7**, 129–135.

Noebels JL & Sidman RL (1979). Inherited epilepsy: spike-wave and focal motor seizures in the mutant mouse tottering. *Science* **204**, 1334–1336.

Onslow ACE, Jones MW & Bogacz R (2014). A canonical circuit for generating phase-amplitude coupling. *PloS One* **9**, e102591.

Özkurt TE & Schnitzler A (2011). A critical note on the definition of phase-amplitude cross-frequency coupling. *J Neurosci Methods* **201**, 438–443.

Penny WD, Duzel E, Miller KJ & Ojemann JG (2008). Testing for nested oscillation. *J Neurosci Methods* **174**, 50–61.

Rossignol E, Kruglikov I, van den Maagdenberg AMJM, Rudy B & Fishell G (2013). Ca$_V$2.1 ablation in cortical interneurons selectively impairs fast-spiking basket cells and causes generalized seizures. *Ann Neurol* **74**, 209–222.

Scheffer-Teixeira R, Belchior H, Leão RN, Ribeiro S & Tort ABL (2013). On high-frequency field oscillations (>100 Hz) and the spectral leakage of spiking activity. *J Neurosci* **33**, 1535–1539.

Scheffzük C, Kukushka VI, Vyssotski AL, Draguhn A, Tort ABL & Brankačk J (2011). Selective coupling between theta phase and neocortical fast gamma oscillations during REM-sleep in mice. *PloS One* **6**, e28489.

Smyk MK, Coenen AML, Lewandowski MH & van Luijtelaar G (2011). Endogenous rhythm of absence epilepsy: relationship with general motor activity and sleep-wake states. *Epilepsy Res* **93**, 120–127.

Sotero RC (2015). Modeling the generation of phase-amplitude coupling in cortical circuits: from detailed networks to neural mass models. *Biomed Res Int* **2015**, 915606.

Szczepanski SM, Crone NE, Kuperman RA, Auguste KI, Parvizi J & Knight RT (2014). Dynamic changes in phase-amplitude coupling facilitate spatial attention control in fronto-parietal cortex. *PLoS Biol* **12**, e1001936.

Tadel F, Baillet S, Mosher JC, Pantazis D & Leahy RM (2011). Brainstorm: a user-friendly application for MEG/EEG analysis. *Comput Intell Neurosci* **2011**, 879716.

Tort ABL, Komorowski R, Eichenbaum H & Kopell N (2010). Measuring phase-amplitude coupling between neuronal oscillations of different frequencies. *J Neurophysiol* **104**, 1195–1210.

Voytek B, Canolty RT, Shestyuk A, Crone NE, Parvizi J & Knight RT (2010). Shifts in gamma phase-amplitude coupling frequency from theta to alpha over posterior cortex during visual tasks. *Front Hum Neurosci* **4**, 191.

Wulff P, Ponomarenko AA, Bartos M, Korotkova TM, Fuchs EC, Bähner F, Both M, Tort ABL, Kopell NJ, Wisden W & Monyer H (2009). Hippocampal theta rhythm and its coupling with gamma oscillations require fast inhibition onto parvalbumin-positive interneurons. *Proc Natl Acad Sci USA* **106**, 3561–3566.

Xiang J, Tenney JR, Korman AM, Leiken K, Rose DF, Harris E, Yuan W, Horn PS, Holland K, Loring DW & Glauser TA (2014). Quantification of interictal neuromagnetic activity in absence epilepsy with accumulated source imaging. *Brain Topogr* **28**, 904–914.

Zhang X, Zhong W, Brankačk J, Weyer SW, Müller UC, Tort ABL & Draguhn A (2016). Impaired theta-gamma coupling in APP-deficient mice. *Sci Rep* **6**, 21948.

Additional information

Competing interests

There are no conflicts of interest for any of the authors.

Author contributions

A.M. conceived and designed the work; A.M., I.A., M.W., R.M., K.Y. and S.P. acquired, analysed and interpreted the data; B.L.F. and J.L.N. analysed and interpreted the data. All authors revised the work critically for important intellectual content, approved the final version of the manuscript, and agreed to be accountable for all aspects of the work in ensuring that questions related to the accuracy or integrity of any part of the work were appropriately investigated and resolved. Al persons designated as authors qualify for authorship, and all those who qualify for authorship are listed.

Funding

Translational perspective

Patients with epilepsy frequently have comorbidities that may persist despite successful treatment of seizures, but the current focus of clinical EEG is limited to detection of the presence or absence of epileptiform activity. With an appropriate sampling rate, careful attention to patients' state of arousal, and selection of epochs free from myogenic artefact, the work presented here suggests that quantitative analysis of features encoded in human scalp EEG, such as phase–amplitude coupling, may serve as a biomarker for cognitive deficits, which may then be treated in parallel with seizures. Further behavioural studies in rodents and humans with simultaneous intracranial and scalp EEG will be necessary to validate this hypothesis.